

# Supporting Information

## An Enantiopure Fe<sup>III</sup><sub>4</sub> Single Molecule Magnet

Yuan-Yuan Zhu, Xiao Guo, Chang Cui, Bing-Wu Wang\*, Zhe-Ming Wang, and  
Song Gao\*

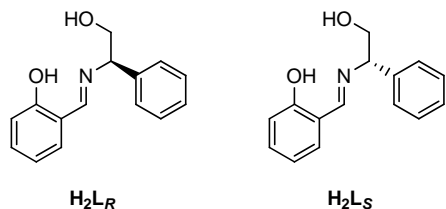
### Physical measurement

Magnetic measurements were performed on a Quantum Design MPMS XL-5 SQUID magnetometer on polycrystalline samples. Data were corrected for the diamagnetism of the samples using Pascal constants and of the sample holder by measurement. The experiments below 1.8 K were measured on the *i*Helium Measurement Console in coordination with MPMS MultiVu.

The X-ray measurements of **1R** were carried on a Saturn724+ CCD diffractometer with graphite-monochromator Mo-K $\alpha$  radiation ( $\lambda = 0.71073 \text{ \AA}$ ) at 173 K. Intensities were collected using CrystalClear (Rigaku Inc., 2008) technique and absorption effects were collected using the Numerical technique. The X-ray measurements of **1S** were carried on a Saturn724+ CCD diffractometer with Confocal-monochromator Mo-K $\alpha$  radiation ( $\lambda = 0.71073 \text{ \AA}$ ) at 173 K. Intensities were collected using CrystalClear (Rigaku Inc., 2008) technique and absorption effects were collected using the multi-scan technique. The structure of **1R** and **1S** was solved using SHELXS-97 program<sup>1</sup> and refined by a full matrix least squares technique based on  $F^2$  using SHELXL 97 program.<sup>2</sup>

CD spectral measurements in solution and solid state were performed on a JASCO J-815 CD spectropolarimeter. The CD spectra were calculated with the TDDFT method at the B3LYP/6-31G\* level of theory for three model fragment structures of **1R**. Hydrogen atoms were added theoretically to balance the charge. The standard Pople style basis sets, 6-31G with one set of 'd-' polarization functions on

non-hydrogen atoms are used in the calculations. All the computations were performed in the Gaussian 09 package.<sup>3</sup>

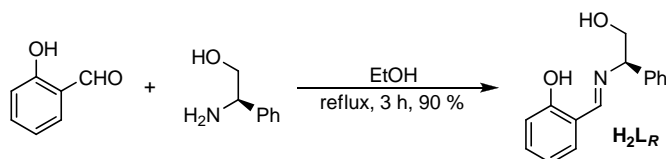


**Scheme S1** The structure of the ligands  $\text{H}_2\text{L}_R$  and  $\text{H}_2\text{L}_S$ .

## Synthesis

All starting materials were purchased as reagent grade and were used without further purification.

### Synthesis of the Schiff base ligands



**Compound  $\text{H}_2\text{L}_R$ .** A solution of salicylaldehyde (1.56 g, 10.0 mmol) and (*R*)-2-amino-2-phenylethanol (1.37 g, 10.0 mmol) in ethanol was stirred under reflux for 2 h and the color of the solution was turned to yellow. After removal of the solvents under reduced pressure, the crude product was purified by recrystallization in the mixture solvent of ethanol and petroleum ether to give compound  $\text{L}_R$  as needlelike crystals (2.17 g, 90 %).  $^1\text{H}$  NMR (400 MHz,  $\text{CDCl}_3$ ):  $\delta$  13.30 (br, 1 H), 8.48 (s, 1 H), 7.38-7.26 (m, 9 H), 6.98 (d,  $J = 8.2$  Hz, 1 H), 6.89 (t d,  $J_1 = 7.4$  Hz,  $J_2 = 1.2$  Hz, 1 H), 4.47 (t,  $J = 6.5$  Hz, 1 H), 3.92 (d,  $J = 7.0$  Hz, 2 H). Anal. Calcd for  $\text{C}_{15}\text{H}_{15}\text{NO}_2$ : C, 74.67; H, 6.27; N, 5.81. Found: C, 74.65; H, 6.52; N, 5.73. IR (pure sample):  $\nu = 3225(\text{m}), 3088(\text{w}), 3031(\text{w}), 3008(\text{w}), 2970(\text{w}), 2952(\text{w}), 2930(\text{w}), 2920(\text{w}), 2863(\text{w}), 2734(\text{w}), 2664(\text{w}), 1949(\text{w}), 1924, 1871(\text{w}), 1802(\text{w}), 1747(\text{w}), 1690(\text{w}), 1626(\text{s}), 1581(\text{m}), 1494(\text{m}), 1462(\text{m}), 1410(\text{m}), 1383(\text{m}), 1359(\text{w}), 1338(\text{w}), 1317(\text{w}), 1275(\text{s}), 1213(\text{w}), 1155(\text{m}), 1120(\text{w}), 1080(\text{m}), 1064(\text{m}), 1044(\text{m}), 1031(\text{m}), 1003(\text{w}), 979(\text{w}),$

942(w), 918(w), 905(w), 891(w), 872(w), 853(w), 809(w), 772(m), 764(m), 756(m), 740(w), 694(m), 639(w).

The enantiomer compound **H<sub>2</sub>L<sub>S</sub>** was synthesized by using salicylaldehyde and (*S*)-2-amino-2-phenylethanol as start materials in the same way. <sup>1</sup>H NMR (400 MHz, CDCl<sub>3</sub>): δ 13.32 (br, 1 H), 8.47 (s, 1 H), 7.40-7.25 (m, 9 H), 6.97 (d, *J* = 8.4 Hz, 1 H), 6.88 (t d, *J*<sub>1</sub> = 7.4 Hz, *J*<sub>2</sub> = 1.2 Hz, 1 H), 4.46 (t, *J* = 6.4 Hz, 1 H), 3.91 (d, *J* = 7.6 Hz, 2 H). Anal. Calcd for C<sub>15</sub>H<sub>15</sub>NO<sub>2</sub>: C, 74.67; H, 6.27; N, 5.81. Found: C, 74.68; H, 6.51; N, 5.79. IR (pure sample): ν = 3224(m), 3088(w), 3031(w), 3008(w), 2970(w), 2952(w), 2930(w), 2920(w), 2863(w), 2734(w), 2664(w), 1949(w), 1924(w), 1871(w), 1802(w), 1747(w), 1690(w), 1626(s), 1581(m), 1494(m), 1462(m), 1410(m), 1383(m), 1359(w), 1338(w), 1317(w), 1275(s), 1213(w), 1155(m), 1120(w), 1080(m), 1064(m), 1044(m), 1031(m), 1003(w), 979(w), 942(w), 918(w), 905(w), 891(w), 872(w), 853(w), 809(w), 772(m), 764(m), 756(m), 740(w), 694(m), 639(w).

### Synthesis of the compounds **1R** and **1S**

**Compound 1R.** ([Fe<sub>4</sub>(L<sub>R</sub>)<sub>6</sub>]·5DMF·H<sub>2</sub>O): A mixture of H<sub>2</sub>L<sub>R</sub> (362 mg, 1.5 mmol) and Et<sub>3</sub>N (4.3 mL, 3 mmol) in methanol (20 mL) was stirred at room temperature. A brown precipitate was generated as soon as the solution of FeCl<sub>2</sub> (198 mg, 1 mmol) in methanol (10 mL) was added dropwise (the Fe ions were oxidated from +2 valence to +3 valence in the air immediately), and the mixture was stirred at room temperature for 12 h. The resulting solution was filtered and the solvent was removed under vacuum. The brown precipitate obtained was dried under vacuum then redissolved in hot DMF (40 mL). Dark brown chunks were obtained within two weeks in 70-80 % yield by slow evaporation of the resulting solution. The crystals are stable at room temperature and no loss of solvent is observed. Anal. Calcd for C<sub>105</sub>H<sub>109</sub>Fe<sub>4</sub>N<sub>11</sub>O<sub>8</sub>: C, 61.93; H, 5.39; N, 7.57. Found: C, 61.80; H, 5.59; N, 7.55. IR (pure sample): ν = 3061(w), 3027(w), 2927(w), 2859(w), 1678(m), 1624(s), 1600(m), 1541(m), 1493(w), 1468(m), 1452(m), 1443(m), 1385(m), 1360(w), 1340(m), 1315(m), 1252(w), 1216(w), 1197(m), 1149(m), 1126(w), 1089(w), 1069(m), 1043(m), 1030(m),

1002(w), 986(w), 943(m), 900(m), 853(w), 827(w), 803(w), 757(m), 738(w), 703(m), 658(w), 637(w), 607(w).

The enantiomer complexes of **1S** ( $[\text{Fe}_4(\text{L}_S)_6] \cdot 5\text{DMF} \cdot \text{H}_2\text{O}$ ) was synthesized by using  $\text{H}_2\text{L}_S$  as ligand in the same way. Anal. Calcd for  $\text{C}_{105}\text{H}_{109}\text{Fe}_4\text{N}_{11}\text{O}_8$ : C, 61.93; H, 5.39; N, 7.57. Found: C, 62.00; H, 5.55; N, 7.51. IR (pure sample):  $\nu = 3061(\text{w}), 3027(\text{w}), 2928(\text{w}), 2859(\text{w}), 1677(\text{m}), 1625(\text{s}), 1600(\text{m}), 1541(\text{m}), 1493(\text{w}), 1469(\text{m}), 1452(\text{m}), 1443(\text{m}), 1386(\text{m}), 1361(\text{w}), 1340(\text{m}), 1315(\text{m}), 1254(\text{w}), 1217(\text{w}), 1198(\text{m}), 1149(\text{m}), 1126(\text{w}), 1089(\text{w}), 1069(\text{m}), 1043(\text{m}), 1030(\text{m}), 1002(\text{w}), 986(\text{w}), 943(\text{w}), 901(\text{w}), 853(\text{w}), 828(\text{w}), 803(\text{w}), 759(\text{m}), 738(\text{w}), 704(\text{m}), 658(\text{w}), 637(\text{w}), 607(\text{w})$ .  
 $(\text{H}_2\text{L}_R = (\text{R})\text{-}2\text{-}((2\text{-hydroxy-1-phenylethylimino methyl)phenol}), \text{H}_2\text{L}_S = (\text{S})\text{-}2\text{-}((2\text{-hydroxy-1-phenylethylimino)methyl)phenol)$

## References

1. Sheldrick, G. M. *SHELXS-97*; University of Gottingen: Gottingen, Germany, 1990.
2. Sheldrick, G. M. *SHELXS-97*; University of Gottingen: Gottingen, Germany, 1997.
3. Gaussian 09, Revision A.1, M. J. Frisch, G. W. Trucks, H. B. Schlegel, G. E. Scuseria, M. A. Robb, J. R. Cheeseman, G. Scalmani, V. Barone, B. Mennucci, G. A. Petersson, H. Nakatsuji, M. Caricato, X. Li, H. P. Hratchian, A. F. Izmaylov, J. Bloino, G. Zheng, J. L. Sonnenberg, M. Hada, M. Ehara, K. Toyota, R. Fukuda, J. Hasegawa, M. Ishida, T. Nakajima, Y. Honda, O. Kitao, H. Nakai, T. Vreven, J. A. Montgomery, Jr., J. E. Peralta, F. Ogliaro, M. Bearpark, J. J. Heyd, E. Brothers, K. N. Kudin, V. N. Staroverov, R. Kobayashi, J. Normand, K. Raghavachari, A. Rendell, J. C. Burant, S. S. Iyengar, J. Tomasi, M. Cossi, N. Rega, J. M. Millam, M. Klene, J. E. Knox, J. B. Cross, V. Bakken, C. Adamo, J. Jaramillo, R. Gomperts, R. E. Stratmann, O. Yazyev, A. J. Austin, R. Cammi, C. Pomelli, J. W. Ochterski, R. L. Martin, K. Morokuma, V. G. Zakrzewski, G. A. Voth, P. Salvador, J. J. Dannenberg, S. Dapprich, A. D. Daniels, Ö. Farkas, J. B. Foresman, J. V. Ortiz, J. Cioslowski, and D. J. Fox, Gaussian, Inc., Wallingford CT, 2009.

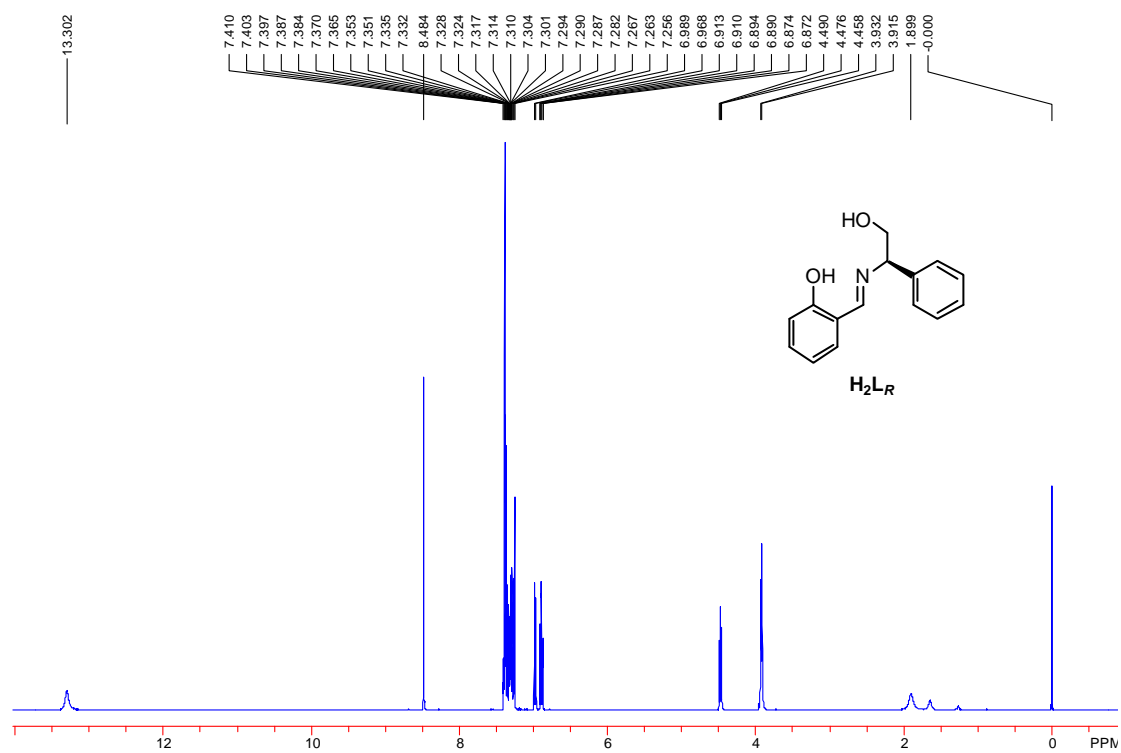


**Figure S1.** <sup>1</sup>H NMR spectrum of **H<sub>2</sub>L<sub>R</sub>** (400 MHz) in CDCl<sub>3</sub> (10 mM).

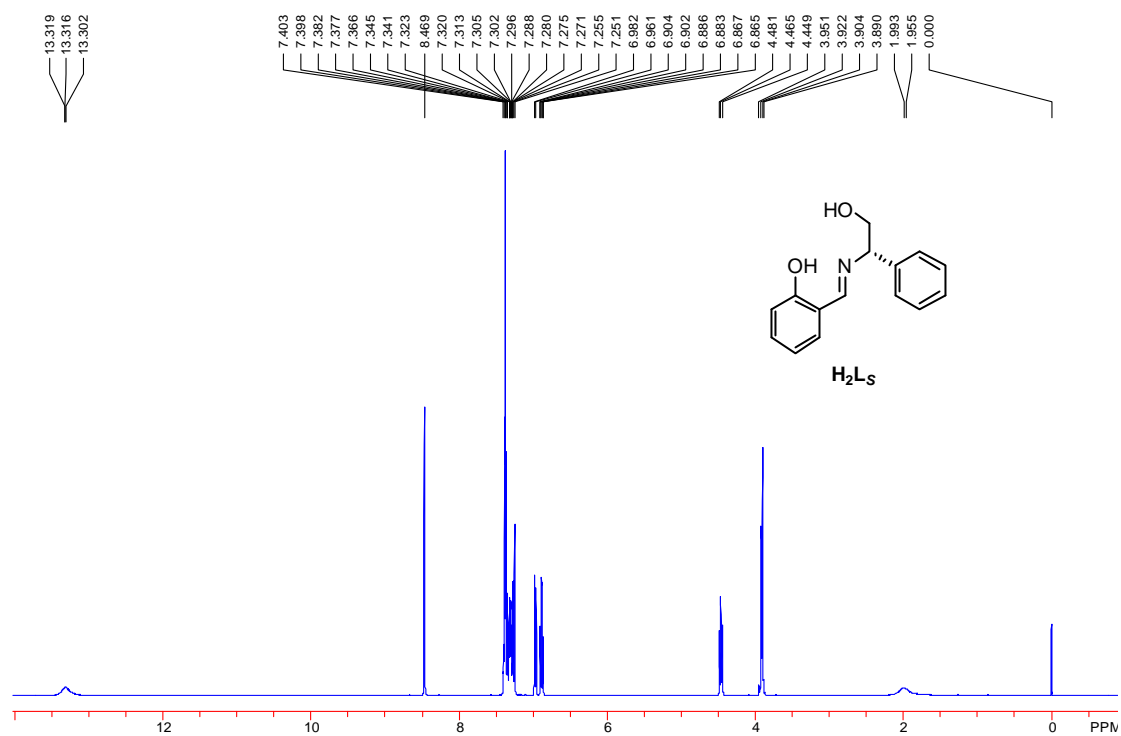


**Figure S2.** <sup>1</sup>H NMR spectrum of **H<sub>2</sub>L<sub>S</sub>** (400 MHz) in CDCl<sub>3</sub> (10 mM).

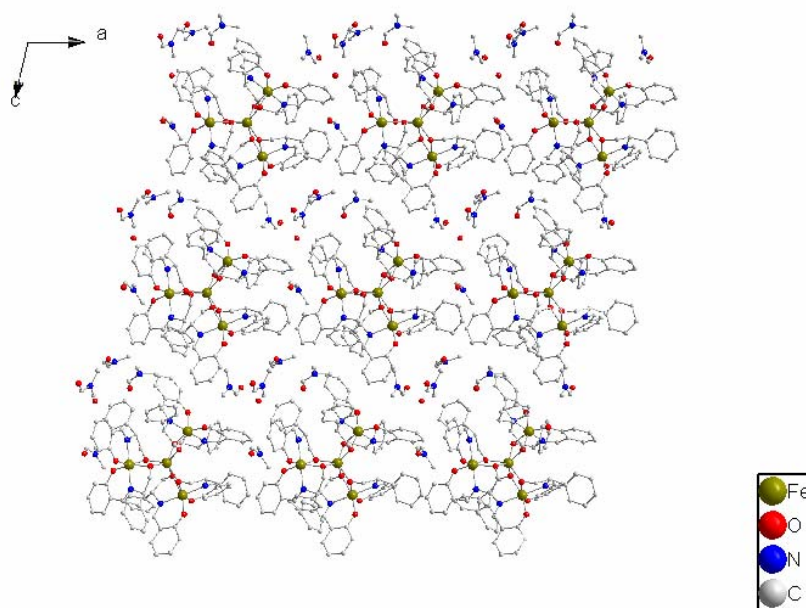


**Figure S3.** View of the crystal packing of **1R** along *b* axis.

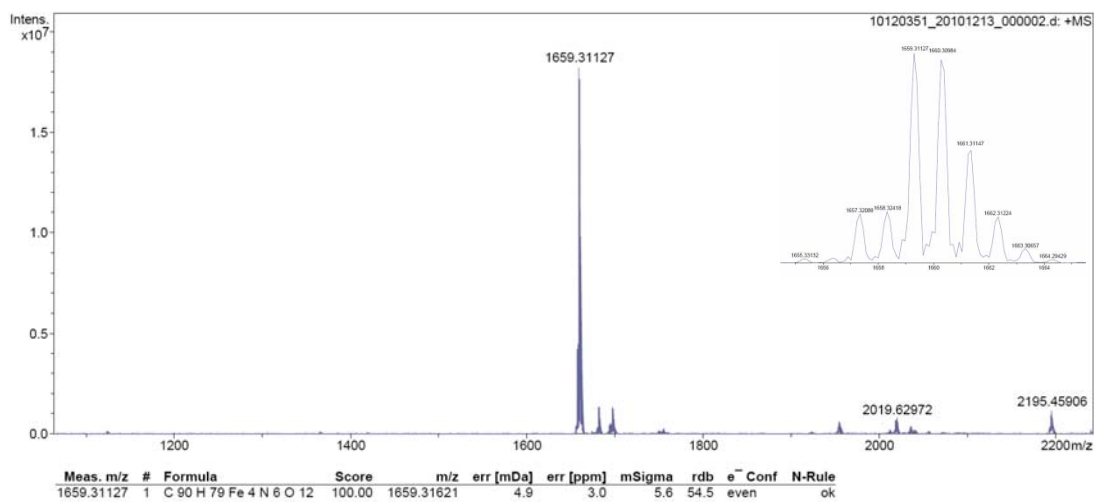


**Figure S4.** Positive-mode high resolution ESI-MS spectrum of **1R**. The inset shows the expand ion signal at  $m/z = 1659.3$  attributable to the  $[\mathbf{1R} + \text{H}]^+$  ion.

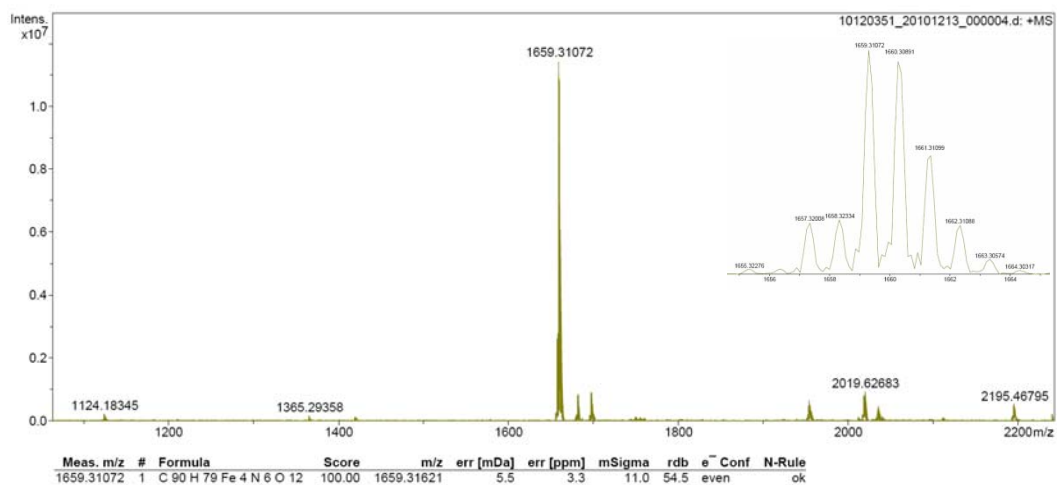


**Figure S5.** Positive-mode high resolution ESI-MS spectrum of **1S**. The inset shows the expand ion signal at  $m/z = 1659.3$  attributable to the  $[1S + H]^+$  ion.

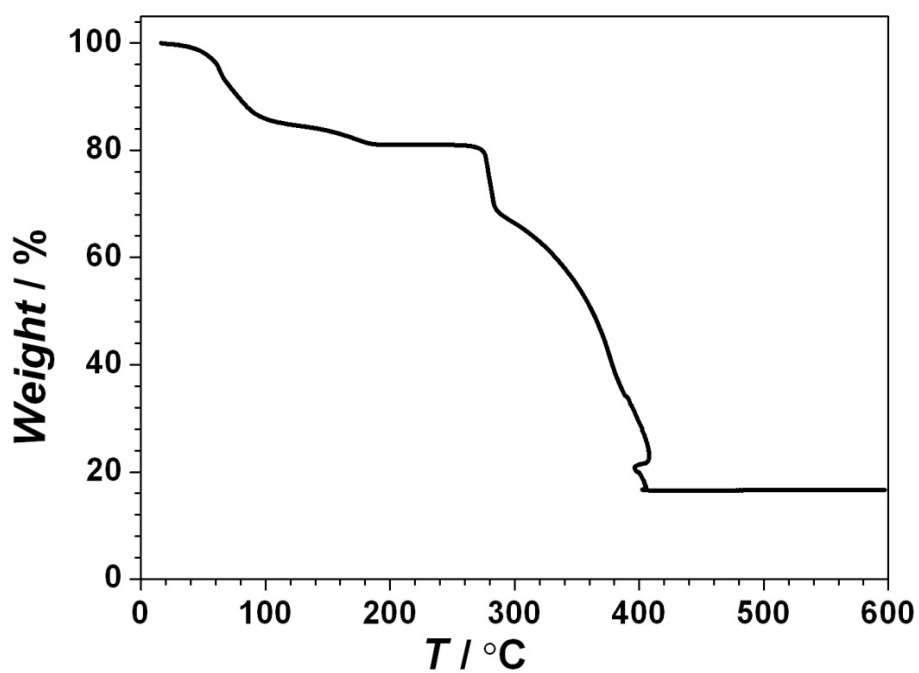


**Figure S6.** The TGA traces for **1R**.

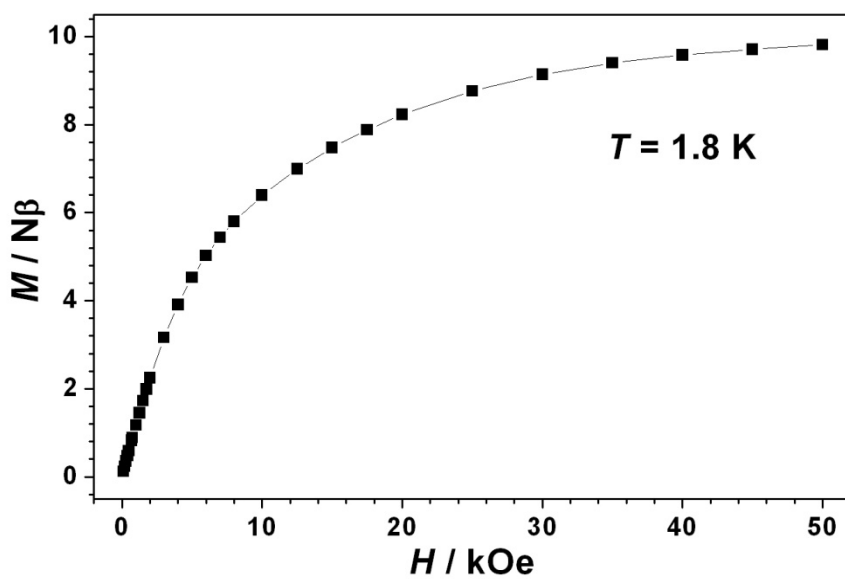


*Figure S7.*  $M$  vs  $H$  plot at 1.8 K for **1R** from 0 to 50 kOe.

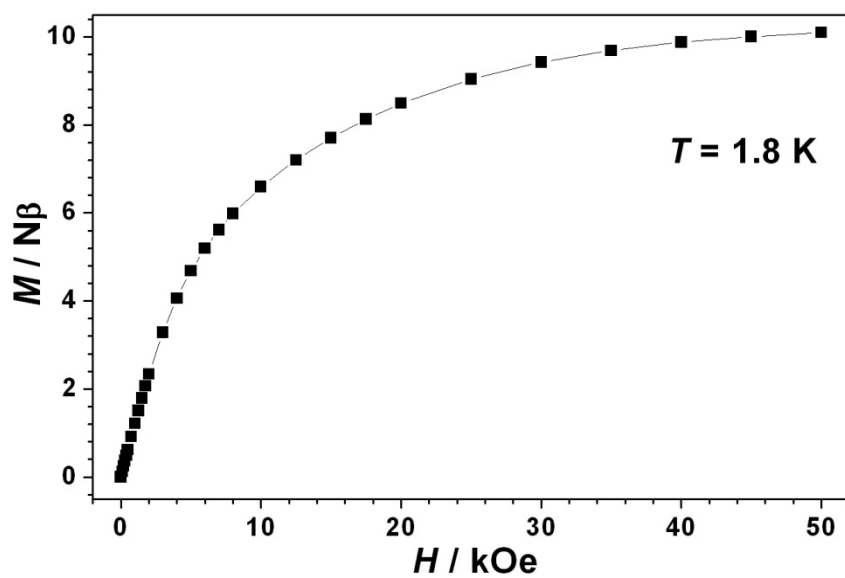


*Figure S8.*  $M$  vs  $H$  plot at 1.8 K for **1S** from 0 to 50 kOe.

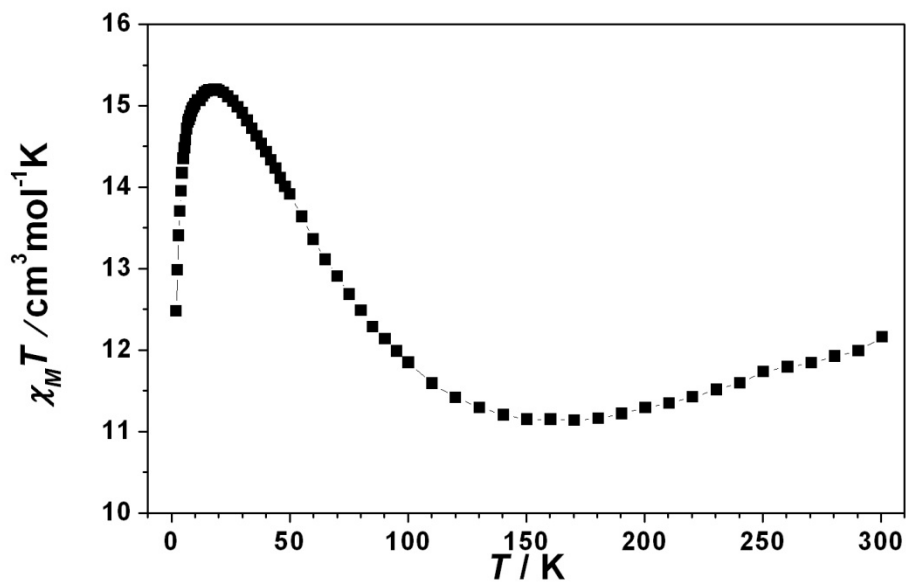


*Figure S9.* Temperature dependence of  $\chi_M T$  of **1S** at  $H = 1$  kOe from 2-300 K.

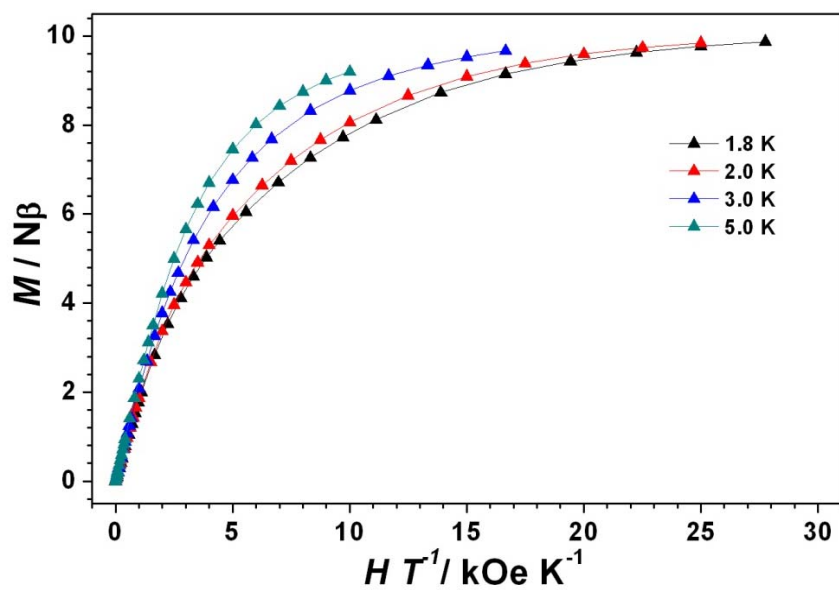


*Figure S10.*  $M$  vs  $H/T$  plots at different temperature (1.8 K, 2.0 K, 3.0 K, and 5.0 K) of **1R**.

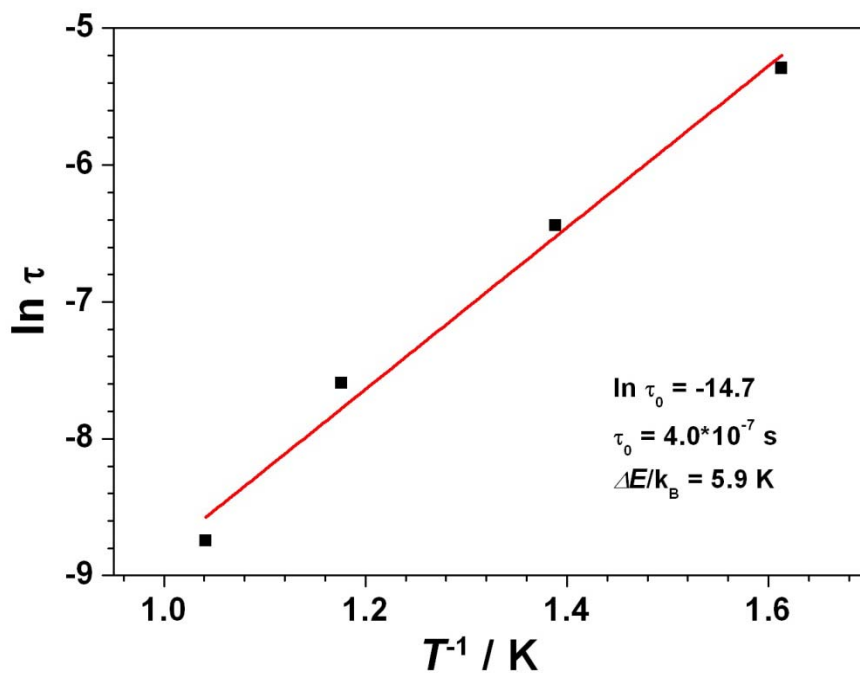


**Figure S11.** Relaxation time ( $\ln \tau$ ) versus  $1/T$  (ac susceptibility in 0 Oe). The solid line corresponds to the linear fit by using least squares method showing an Arrhenius-type behavior.

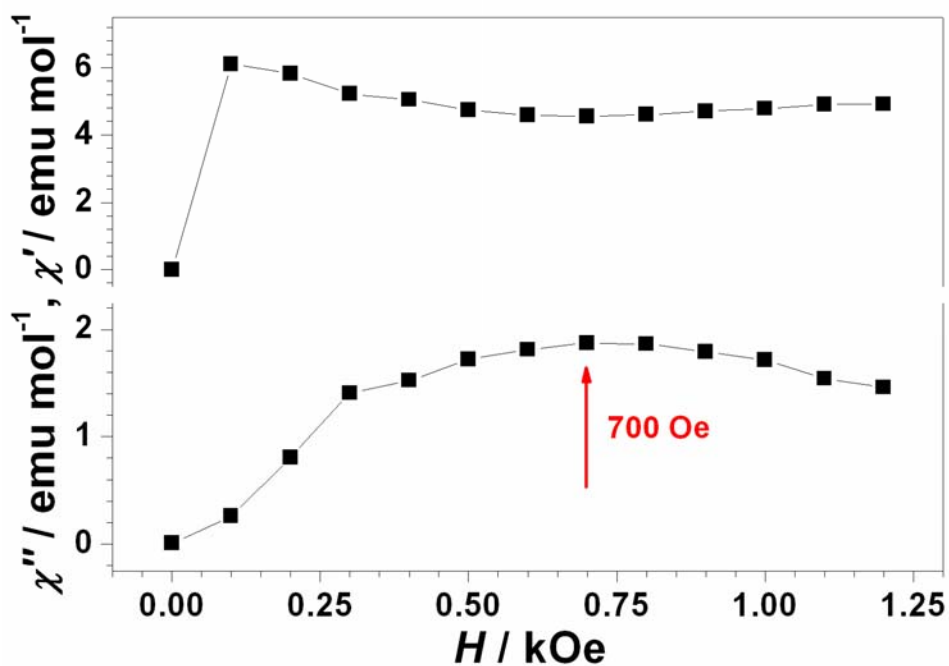


**Figure S12.** The field dependence of ac susceptibility at 2.0 K (frequency = 10 Hz), the maximum of out-of-phase ( $\chi''$ ) susceptibility emerges in 700 Oe.

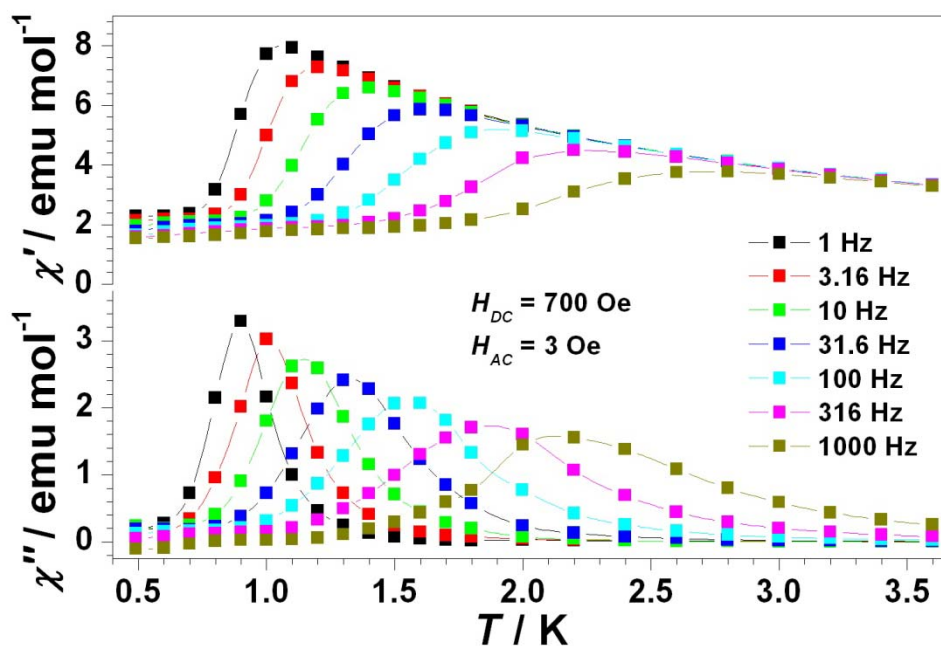


**Figure S13.** The temperature dependence of ac susceptibility in 700 Oe applied static field with an oscillating field of 3 Oe at frequencies from 1 to 1000 Hz for **1R**.

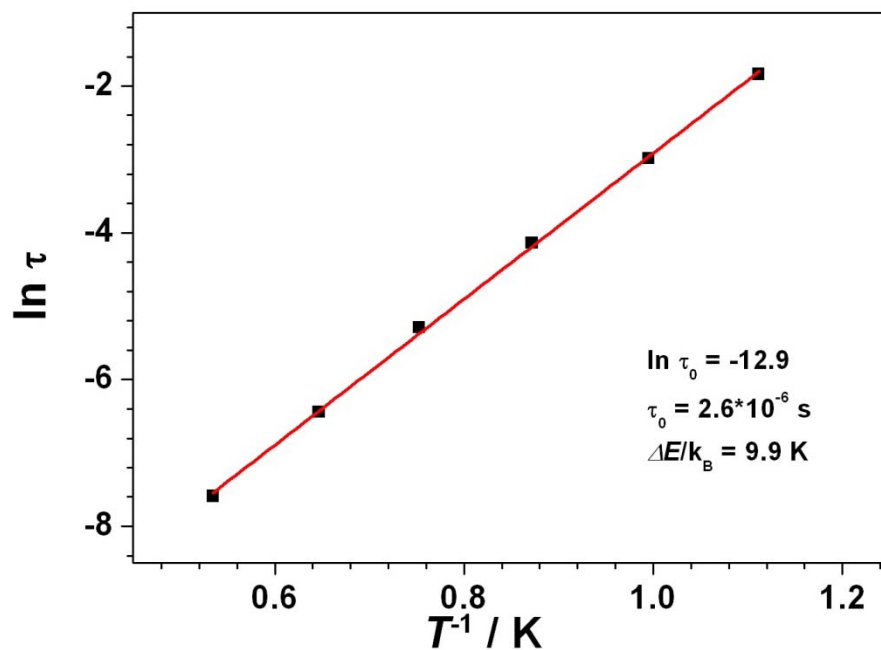


**Figure S14.** Relaxation time ( $\ln \tau$ ) versus  $1/T$  (ac susceptibility in 700 Oe). The solid line corresponds to the linear fit by using least squares method showing an Arrhenius-type behavior.

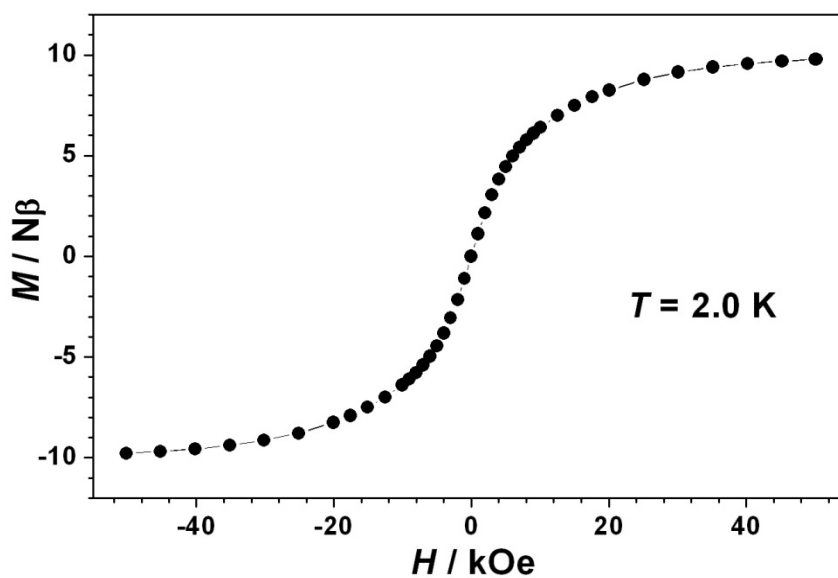


**Figure S15.** Magnetization versus field measured for the **1R** at 2.0 K from -50 kOe to 5 kOe, no hysteresis loop was observed.

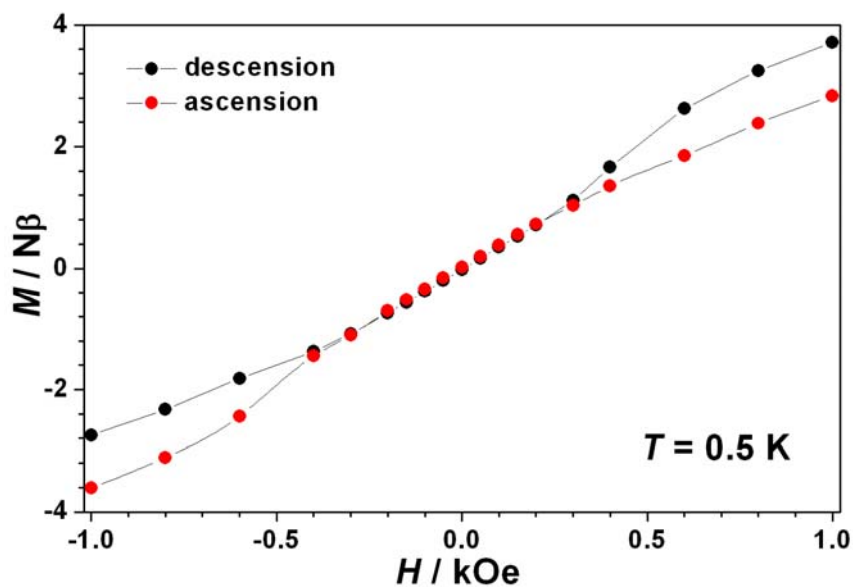


**Figure S16.** A zoom of the butterfly-shaped hysteresis loop close to 0 Oe at 0.5 K for the polycrystalline sample of **1R**.

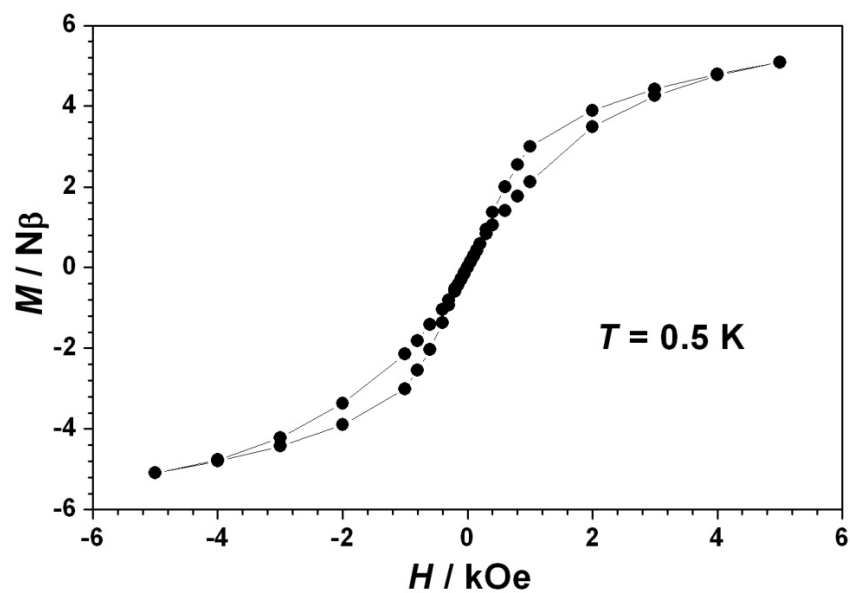


**Figure S17.** Butterfly-shaped hysteresis loop for the **1S** at 0.5 K.

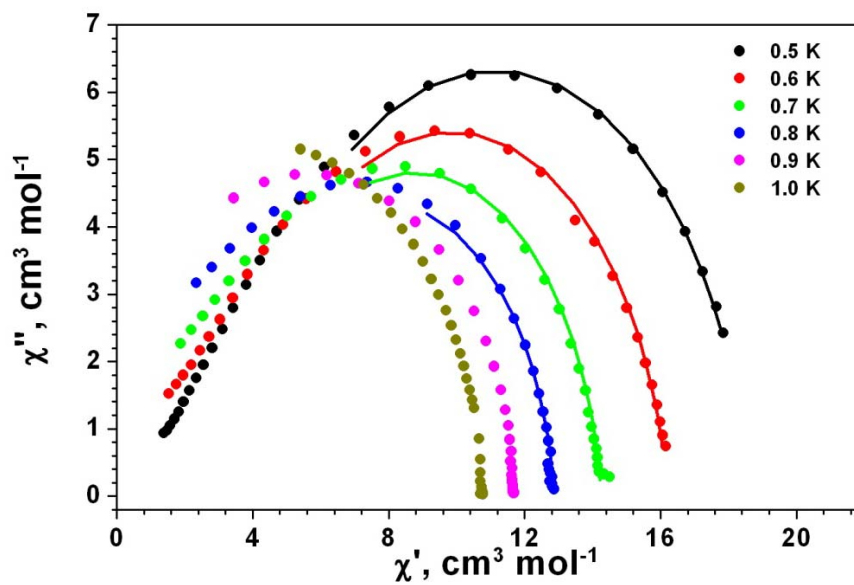


**Figure S18.** Cole-Cole diagram of **1R** at 0.5, 0.6, 0.7, 0.8, 0.9, and 1.0 K with zero applied dc field.

Ref: (a) K. S. Cole, R. H. Cole, *J. Chem. Phys.* 1941, **9**, 341. (b) S. M. Aubin, Z. Sun, L. Pardi, J. Krzysteck, K. Folting, L.-J. Brunel, A. L. Rheingold, G. Christou, D. N. Hendrickson, *Inorg. Chem.* 1999, **38**, 5329.

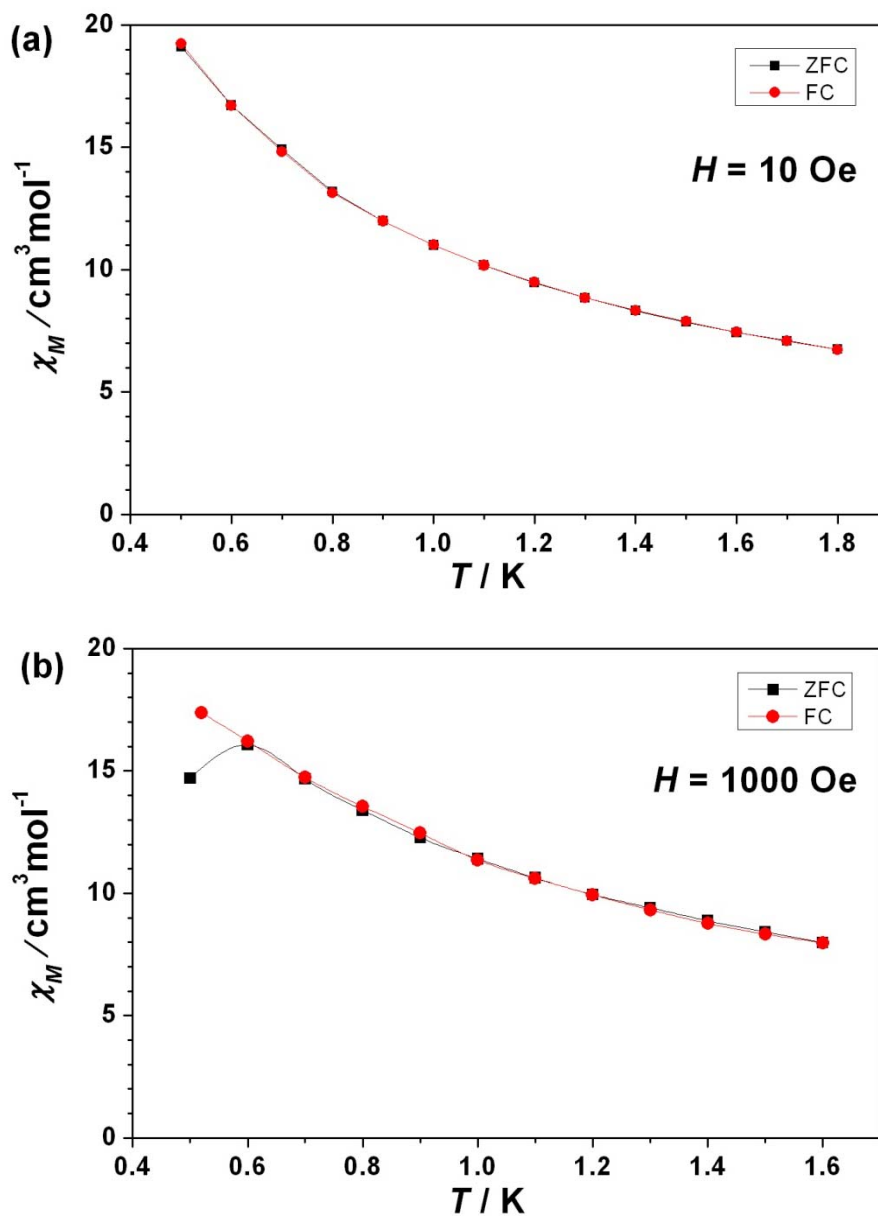


**Figure S19.** Plots of zero-field cooled magnetization (ZFC) and field-cooled magnetization (FC) and in fields of (a) 10 Oe and (b) 1000 Oe for **1R**.

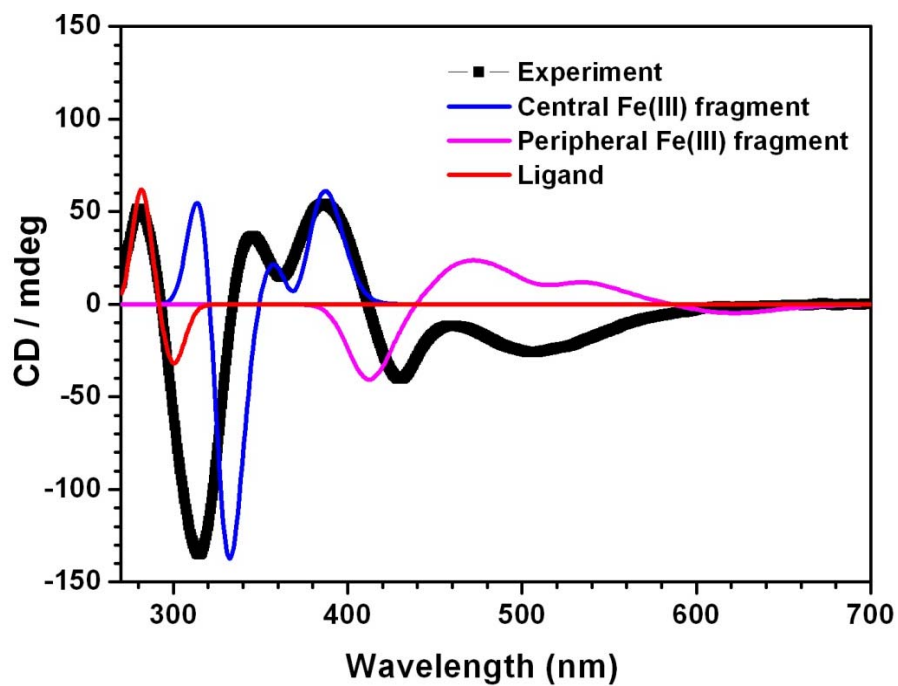


**Figure S20.** The experimental CD spectra for **1R** and calculated ones for central and peripheral Fe(III) fragment, ligand computed at B3LYP/6-31G\* level of theory.

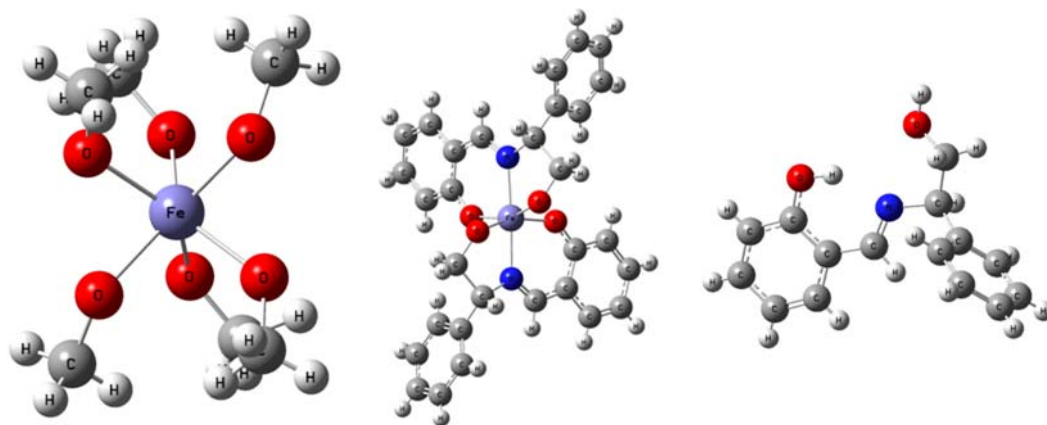


**Figure S21.** Model structures for the (a) central Fe(III) fragment, (b) peripheral Fe(III) fragment and (c) ligand.

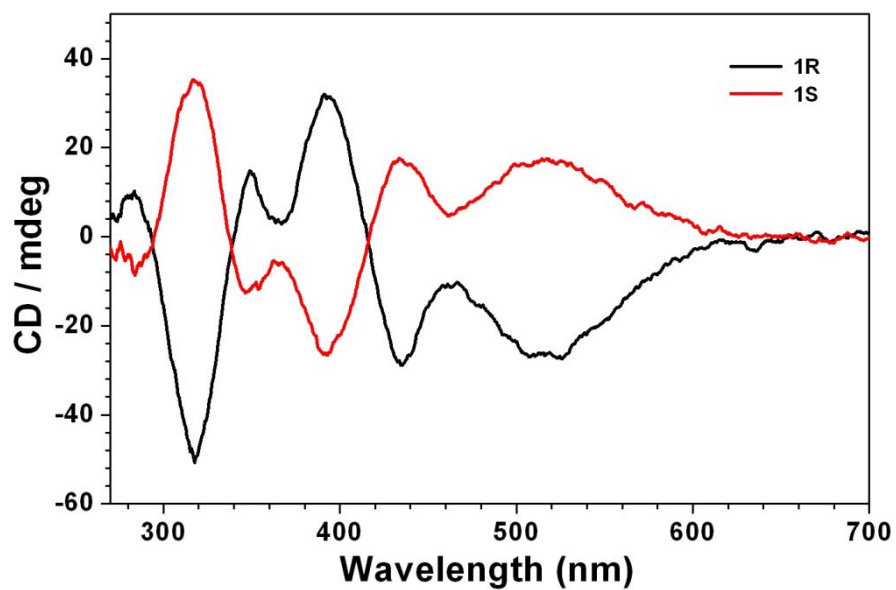


**Figure S22.** The solid-state CD spectra of **1R** (black) and **1S** (red) in KBr pellet at 298 K.